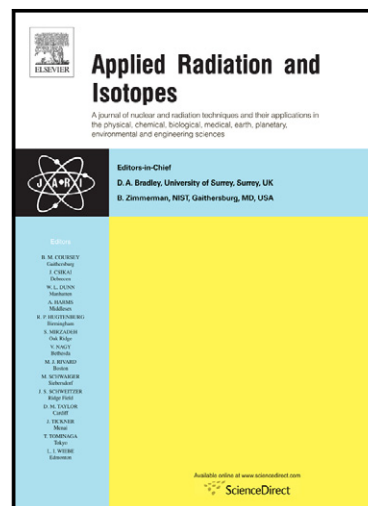


# Author's Accepted Manuscript

## Radiosynthesis and *in vivo* Evaluation of a $^{18}\text{F}$ -Labelled Styryl-Benzoxazole Derivative for $\beta$ -Amyloid Targeting

G.Ribeiro Morais, L. Gano, T. Kniess, R. Bergmann, A. Abrunhosa, I. Santos, A. Paulo



[www.elsevier.com/locate/apradiso](http://www.elsevier.com/locate/apradiso)

PII: S0969-8043(13)00292-3  
DOI: <http://dx.doi.org/10.1016/j.apradiso.2013.07.003>  
Reference: ARI6294

To appear in: *Applied Radiation and Isotopes*

Received date: 9 January 2013  
Revised date: 15 April 2013  
Accepted date: 1 July 2013

Cite this article as: G.Ribeiro Morais, L. Gano, T. Kniess, R. Bergmann, A. Abrunhosa, I. Santos, A. Paulo, Radiosynthesis and *in vivo* Evaluation of a  $^{18}\text{F}$ -Labelled Styryl-Benzoxazole Derivative for  $\beta$ -Amyloid Targeting, *Applied Radiation and Isotopes*, <http://dx.doi.org/10.1016/j.apradiso.2013.07.003>

This is a PDF file of an unedited manuscript that has been accepted for publication. As a service to our customers we are providing this early version of the manuscript. The manuscript will undergo copyediting, typesetting, and review of the resulting galley proof before it is published in its final citable form. Please note that during the production process errors may be discovered which could affect the content, and all legal disclaimers that apply to the journal pertain.

**Radiosynthesis and *in vivo* Evaluation of a  $^{18}\text{F}$ -Labelled Styryl-Benzoxazole  
Derivative for  $\beta$ -Amyloid Targeting**

G. Ribeiro Morais,<sup>1</sup> L. Gano,<sup>1</sup> T. Kniess,<sup>2</sup> R. Bergmann,<sup>2</sup> A. Abrunhosa,<sup>3</sup> I. Santos,<sup>1</sup>  
and A. Paulo<sup>1\*</sup>

<sup>1</sup>*Radiopharmaceutical Sciences Group, IST/ITN, Instituto Superior Técnico,  
Universidade Técnica de Lisboa, EN 10, 2686-953 Sacavem;*

<sup>2</sup>*Institute of Radiopharmacy, Helmholtz-Zentrum Dresden-Rossendorf e.V., POB  
510119, D-01314 Dresden, Germany;*

<sup>3</sup>*Universidade Coimbra, ICNAS, Inst Nucl Sci Appl Saúde, P-3000 Coimbra, Portugal*

Corresponding e-mail: [apaulo@itn.pt](mailto:apaulo@itn.pt)

**Keywords:** Alzheimer's Disease/  $\beta$ -Amyloid aggregation/ Molecular Imaging /  
Fluorine-18

**Abstract**

The formation of  $\beta$ -amyloid deposits is considered a histopathological feature of Alzheimer's disease (AD). *In vivo* molecular imaging by means of amyloid-avid radiotracers will allow for an early and conclusive diagnostic of AD. Herein, we describe the radiosynthesis of the radiofluorinated styryl benzoxazole derivative [ $^{18}\text{F}$ ]-[2-[*N*-methyl-*N*-(2'-fluoroethyl)-4'-aminostyryl]benzoxazole] ( $^{18}\text{F}$ -1) and its pre-clinical evaluation, including metabolic and biodistribution studies in male Wistar rat.

The *in vivo* biological evaluation of [ $^{18}\text{F}$ ]-**1** showed that this new radiotracer has a moderate brain uptake with a slow brain washout and a poor *in vivo* stability

### Highlights

- Design of a fluorinated styryl benzoxazole derivative for detection of  $\beta$ -amyloid plaques.
- Nucleophilic radiofluorination with readily available [ $^{18}\text{F}$ ]KF.
- Metabolism and biodistribution studies of the radiofluorinated styryl benzoxazole derivative.

### 1. Introduction

Progressive neurodegenerative disorders such as Alzheimer's (AD) or Parkinson's (PD) disease affect millions of persons worldwide and pose a significant impact in public health, especially as more people approach old age. These diseases, known as "protein misfolding diseases" are characterized by the accumulation of insoluble protein deposits like  $\beta$ -amyloid ( $\text{A}\beta$ ), neurofibrillar tangles in AD, and alpha-synuclein ( $\alpha\text{Syn}$ ) in PD. The molecular processes underlying these diseases are still not completely understood, but the deposition of the amyloid deposits is considered an early and specific event in their pathogenesis (Bacskai, Hickey et al. 2003; Irvine, El-Agnaf et al. 2008).

Being available suitable probes for *in vivo* targeting of  $\text{A}\beta$  deposits, the use of molecular imaging modalities is expected to demonstrate the locations and densities of such deposits in the AD brain allowing an early and assertive diagnosis of AD and/or the monitoring of anti-amyloidogenic therapies. Among the available molecular imaging modalities, positron emission tomography (PET) is the best suited to achieve

such goal, particularly based on amyloid-avid molecules radiolabelled with the cyclotron produced radionuclides carbon-11 ( $^{11}\text{C}$ ) and fluorine-18 ( $^{18}\text{F}$ ) (Kung 2012; Lee, Choe et al. 2012; Ribeiro Morais, Paulo et al. 2012).

A good performing PET radiotracer for *in vivo* imaging of amyloid deposits must show a high binding affinity to  $\text{A}\beta$  and a good permeability through the blood brain barrier (BBB), with minimal non-specific retention in the brain. Taking these requisites into consideration, a plethora of small-sized, planar and non-ionic  $^{11}\text{C}$ - and  $^{18}\text{F}$ -labelled molecules have been synthesized and evaluated as radiotracers for *in vivo* detection of  $\text{A}\beta$  deposits in AD-affected brain. From these studies, the Pittsburgh compound B ( $[^{11}\text{C}]\text{PIB}$ ) (Fig 1) emerged as the gold standard PET radiotracer for *in vivo*  $\beta$ -amyloid imaging (Klunk, Engler et al. 2004). However, the short-life of  $^{11}\text{C}$  ( $t_{1/2} = 20.4$  min) limits its use to centers with an on-site cyclotron. Hence, an intense research effort has been done to obtain alternative  $^{18}\text{F}$ -based radioprobes, as the longer half-life ( $t_{1/2} = 110$  min) of  $^{18}\text{F}$  allows for multistep radiosynthesis, longer *in vivo* investigation, and commercial distribution to other clinical PET centers. In recent years, encouraging results have been reported for a few  $^{18}\text{F}$ -labeled compounds (Fig. 1) (Liu, Kepe et al. 2007; Choi, Golding et al. 2009; Jureus, Swahn et al. 2010; Vandenberghe, Van Laere et al. 2010; Barthel, Gertz et al. 2011; Clark, Schneider et al. 2011) that underwent clinical evaluation in humans as  $\text{A}\beta$  imaging agents. One of these agents,  $^{18}\text{F}$ -Florbetapir (Amyvid) has been recently approved by the FDA for clinical use, giving *in vivo* PET images of amyloid deposits in close correlation with results from postmortem histopathological analysis (Clark, Schneider et al. 2011).

Despite this success, there is still room to investigate alternative PET radioprobes for *in vivo* detection of amyloid aggregates, aiming at the finding of best performing compounds with augmented initial brain uptake and with reduced non-specific retention

in the brain. For this purpose, we have designed a novel family of fluorinated styryl benzazole derivatives that interact *in vitro* with amyloid species in the same way as does Thioflavin T, which is a dye used to stain A $\beta$  deposits in post-mortem histopathological studies. In this paper, we report on the radiosynthesis of one of these compounds, [ $^{18}\text{F}$ ]-[2-[*N*-methyl-*N*-(2'-fluoroethyl)-4'-aminostyryl]benzoxazole] ( $^{18}\text{F}$ -**1**), as well as on its *in vivo* evaluation that comprised biodistribution and metabolism studies in rat.

**Figure 1.**

## 2. Experimental Section

### 2.1 Chemistry

The tosylated precursor 2-[*N*-methyl-*N*-(2'-tosyloxyethyl)-4'-aminostyryl]benzoxazole (**3**) and the cold surrogate 2-[*N*-methyl-*N*-(2'-fluoroethyl)-4'-aminostyryl]benzoxazole (**1**) were synthesized according to previously reported (Ribeiro Morais, Miranda et al. 2011). Briefly, 2-benzoxazolymethyltriphenylphosphonium chloride (2.0 g, 4.6 mmol) in benzene (25 mL) was reacted with K<sup>t</sup>BuO (525 mg, 4.7 mmol) at rt. After 3 h, the reaction mixture was diluted with EtOAc (100 mL) and was extracted with water (100 mL). The organic phase was dried over MgSO<sub>4</sub>, filtered and the filtrate was dried under vacuum. Then, the resulting phosphorane was refluxed overnight with *N*-methyl-*N*-(2-tosyloxyethyl)-4 aminobenzaldehyde (590 mg, 1.8 mmol) in anhydrous THF (25 mL). Thereafter, the solvent was concentrated and the reaction crude was re-dissolved in CH<sub>2</sub>Cl<sub>2</sub> (100 mL). The organic phase was extracted with sat. sol. of NaHCO<sub>3</sub> (100 mL). The organic extract was dried over MgSO<sub>4</sub>, filtered and the filtrate was concentrated. Compound **3** (550 mg, 65 %) was purified by column chromatography on silica gel (n-hexane/EtOAc/CHCl<sub>3</sub> 3:1:1). To a solution of **3** (250 mg, 0.55 mmol) in anhydrous THF (23 mL) was added anhydrous TBAF (1.8 mL, 1.8 mmol, 1.0 M in

THF). The reaction mixture was refluxed for 30 minutes. Thereafter the solvent was concentrated; chloroform (50 mL) was added to the residue and was extracted with sat sol NaHCO<sub>3</sub> (50 mL). The organic phase was dried over MgSO<sub>4</sub>, filtered and the filtrate was concentrated. Column chromatographic on silica gel (*n*-hexane/EtOAc 4:1) gave the mixture of **1-Z** and **1-E** (124 mg, 76%).

## 2.2 Radiochemistry

No-carrier-added aqueous [<sup>18</sup>F]fluoride was produced in a CYCLONE 18/9 cyclotron (IBA) by irradiation of [<sup>18</sup>O]H<sub>2</sub>O via the <sup>18</sup>O(p,n)<sup>18</sup>F nuclear reaction. Resolubilization of the aqueous [<sup>18</sup>F]fluoride (0.8–1.0 GBq) was accomplished as described by Coenen et al (Coenen, Klatter et al. 1986) with Kryptofix® 2.2.2 and K<sub>2</sub>CO<sub>3</sub> in a conical vial and azeotropically removing water with acetonitrile in a stream of nitrogen. Finally the dried [<sup>18</sup>F]KF was resolubilized in 500 μL of anhydrous acetonitrile and added to **3** (3.0 mg) in a conical glass vial. The vial was sealed and heated for 20 min at 90°C in an oil bath. After cooling the mixture was subjected to semi-preparative HPLC (Discovery C18, 4.6 x 250 mm, 5μm, Supelco) using isocratic elution with acetonitrile/0.1%TFA (70/30) at a flow rate of 4 mL/min originated by a PU1580 pump (Jasco). The products were monitored by UV detector (UV2075, Jasco) at 254nm and by *gamma*-detection with a scintillation detector (Nuclear Interface).

The radiolabeled product [<sup>18</sup>F]-**1** eluting at 9-10 min was separated, diluted with 30mL of water and the whole solution was subjected to a C18 cartridge (200 mg, LiChrolut). The cartridge was washed with 5 mL of water, after that the radiolabeled product [<sup>18</sup>F]-**1** was eluted with 1mL of ethanol and reconstituted with 8mL of E153 electrolyte infusion solution (140mmol/l Na<sup>+</sup>, 5 mmol/l K<sup>+</sup>, 2.5mmol/l Ca<sup>++</sup>, 1.5mmol/l Mg<sup>++</sup>,

50mmol/l acetate, 103mmol/l Cl<sup>-</sup>, Serumwerk Bernburg AG, Bernburg, Germany). This solution was used for biodistribution experiments and stability studies.

Analytical HPLC analyses of the radiolabeled product [<sup>18</sup>F]-**1** were performed by a Lichrograph® system (Merck-Hitachi) equipped with a L4500 UV detector, a L6200 pump and a scintillation detector Gabi (Raytest) using a C18 column (Luna C18(2), 4.6x250, 5µm) and the indicated isocratic eluent with a flow rate of 1.0 mL/min.

The radiotracer [<sup>18</sup>F]-**1** was synthesized in 70 min total synthesis time in 42% total decay corrected yield from [<sup>18</sup>F]fluoride in > 99% radiochemical purity (both isomers) and a specific activity 7-28 GBq/µmol at end of synthesis.

### 2.3 Metabolite analysis

Male Wistar-Unilever rats (n = 2; body weight 150 ± 12 g) were anesthetized with desflurane (9-10% v/v, 30% oxygen/air). The threshold value for breathing frequency was 65 breaths/min. Animals were put in supine position and placed on a heating pad to maintain body temperature. The spontaneously breathing rats were heparinized with 100 units/kg heparin (Heparin-Natrium 25.000-ratiopharm®, ratiopharm GmbH, Germany) by subcutaneous injection to prevent blood clotting on intravascular catheters. After local anesthesia with lignocain (1%; Xylocitin® loc, mibe, Jena, Germany) into the right groin, a catheter (0.8 mm Umbilical Vessel Catheter, Tyco Healthcare, Tullamore, Ireland) was introduced into the right femoral artery for arterial blood sampling. A second needle catheter (35 G) was placed into a tail vein and was used for [<sup>18</sup>F]-**1** radiotracer injection (39 MBq in 0.5 mL of E153/10% ethanol, infusion 1 mL/min). Arterial blood samples were taken 1.5, 10, 30 and 60 min after injection. Arterial plasma was separated by centrifugation (11.000g x 3min) followed by precipitation of the proteins with methanol (2 volumes to 1 volume plasma) followed by 5 min storage

at -60°C. The clear supernatant separated by centrifugation was used for analysis. The radio-HPLC system (Agilent 1100 series) applied for metabolite analysis was equipped with UV detection (254 nm) and an external radiochemical detector (RAMONA, Raytest GmbH, Straubenhardt, Germany). Analysis was performed on a Zorbax C18 300SB (250 × 9.4 mm; 4 µm) column with an eluent system A (water + 0.1%TFA) and B (acetonitrile + 0.1% TFA) in the following gradient: 5 min 95% A, 10 min to 95% B, 5 min at 95% B and 5 min to 95%A at a flow rate of 3 mL/min.

#### **2.4 Biodistribution studies in Wistar rats**

The animal research committee of the Regierungspräsidium Dresden approved the animal facilities and the experiments according to institutional guidelines and the German animal welfare regulations. The experimental procedure used conforms to the *European Convention for the Protection of Vertebrate Animals used for Experimental and other Scientific Purposes* (ETS No. 123), to the *Deutsches Tierschutzgesetz*, and to the *Guide for the Care and Use of Laboratory Animals* published by the US National Institutes of Health (DHEW Publication No. (NIH) 82-23, Revised 1996, Office of Science and Health Reports, DRR/NIH, Bethesda, MD 20205). The Wistar rats (Wistar Unilever, HsdCpb: Wu, Harlan Winkelmann GmbH, Borchon, Germany, 138±16 g body weight) were housed under standard conditions with free access to standard food and tap water. The biodistribution of [<sup>18</sup>F]-**1** was studied in 7 male rats at 5 min and 8 male rats at 60 min after tracer injection. The animals were anesthetised with Desflurane (Suprane, Baxter Healthcare Corporation Deerfield, IL, USA) (7.0-10.0% v/v in 30% oxygen) and 3-5 MBq radiotracer aliquots were administered in 500 µL electrolyte solution E153 (with 10% ethanol) and into a tail vein. After recovery from anaesthesia rats were again anaesthetized at 5 or 60 min after tracer injection, respectively. Blood

was withdrawn by heart puncture, and the animals were euthanized. Organs and tissues were removed, dried, weighted, and the radioactivity was measured in a cross calibrated well counter (WIZARD, Automatic Gamma Counter, Perkin Elmer, Waltham, Ma, USA) or activimeter (Activimeter Isomed 2000; MCD Nuklear Medizintechnik, Dresden, Germany). The data were decay corrected and normalized to the amount of injected activity calculated from the activity of injection syringes before and after injection and expressed as percentage of injected activity (%ID) or injected activity per gram of tissue (%ID/g). Values are quoted as means  $\pm$  standard deviation (mean  $\pm$  SD) for a group of animals.

### 3. Results and Discussion

Recently, we have introduced new fluorinated styryl benzoxazole (compound **1**) and styryl benzothiazole (compound **2**) derivatives that were synthesized based on a multistep and convergent approach, using the Wittig reaction as a key step to introduce the styryl moiety (Scheme 1) (Ribeiro Morais, Miranda et al. 2011). Compounds **1** and **2** were obtained as mixtures of geometric *E* and *Z* isomers, being the *E* isomer formed preferably in spite of the *Z/E* photoisomerization ability of these compounds. The assessment of the *in vitro* binding affinity of the *E* and *Z* isomers of **1** and **2** towards different types of amyloid fibrils (insulin,  $\alpha$ -synuclein and  $\beta$ -amyloid peptide) has shown that compound **1** displays the highest A $\beta$  binding affinity and selectivity. These studies have also proved that the *Z/E* geometric isomerism has almost no influence on the binding profile of **1** and **2** (Ribeiro Morais, Miranda et al. 2011). Altogether, these data led us to consider **1** the most promising compound to be further evaluated as an amyloid-avid probe for *in vivo* detection of A $\beta$  deposits. Hence, we have studied the

synthesis of the  $^{18}\text{F}$ -labelled counterpart ( $[^{18}\text{F}]\text{-1}$ ) of compound **1** and proceeded with its *in vivo* biological evaluation, as reported in here.

### Scheme 1.

The radiosynthesis of the  $^{18}\text{F}$ -labelled styryl benzoxazole ( $[^{18}\text{F}]\text{-1}$ ) has been done using the tosylated precursor **3** as starting material, using a synthetic methodology similar to that previously reported to obtain the cold congener (**1**) (Ribeiro Morais, Miranda et al. 2011). The optimization of the radiosynthesis involved the study of the influence of the temperature (80-100 °C) and use of different solvents (dimethylformamide vs acetonitrile). Under optimized conditions, the synthesis of  $[^{18}\text{F}]\text{-1}$  was achieved by nucleophilic displacement of the tosylate group with dried  $\text{K}[^{18}\text{F}]$  at 90 °C for 20 min, using acetonitrile as solvent and  $\text{K}_2.2.2/\text{K}_2\text{CO}_3$  to catalyze the reaction (Scheme 2). This combination catalyst, commonly used in radiofluorination reaction, increases the solubility of the fluoride ion and enhances its nucleophilicity (Liu, Zhu et al. 2010). The radiotracer  $[^{18}\text{F}]\text{-1}$  has been purified by semipreparative HPLC using an isocratic elution with acetonitrile/0.1% TFA (70/30). After HPLC purification,  $[^{18}\text{F}]\text{-1}$  has been obtained as a mixture of the two *E* and *Z* isomers, as confirmed by HPLC (Fig. 2). No efforts have been made to separate the two *E* and *Z* isomers of  $[^{18}\text{F}]\text{-1}$  since they have the similar affinity towards  $\text{A}\beta(1\text{-}42)$  aggregates with binding constants of  $4.48\pm 0.38$  and  $5.99\pm 0.56 \mu\text{M}^{-1}$ , respectively (Ribeiro Morais, Miranda et al. 2011). Prior to the biodistribution experiments and stability studies,  $[^{18}\text{F}]\text{-1}$  has been reformulated into an aqueous solution containing 10% of ethanol, using a solid phase extraction (SPE) C18 cartridge to perform the reformulation.  $[^{18}\text{F}]\text{-1}$  was synthesized in an overall 42% decay-corrected radiochemical yield and high radiochemical purity (> 99%, both

isomers) with a specific activity of 7-28 GBq/ $\mu$ mol at end of synthesis. The radiotracer [ $^{18}\text{F}$ ]-**1** was synthesized in 70 min total synthesis time, which included the purification and reformulation. The radiochemical purity was determined based on radio-TLC and analytical HPLC experiments. The chemical identity of compound [ $^{18}\text{F}$ ]-**1** was assessed by HPLC comparison with authentic samples of the *E* and *Z* isomers of the cold congener **1**.

### Scheme 2.

Biodistribution and metabolism studies of [ $^{18}\text{F}$ ]-**1** were performed in male Wistar rats, in order to have a first insight into its potential relevance as a radiotracer for *in vivo* imaging of A $\beta$  aggregates. In particular, these studies intended to elucidate if the compound could cross the BBB with a fast washout from the healthy brain, a crucial issue to reach intra cerebral amyloid deposits with minimal non-specific uptake.

### Figure 2.

The biodistribution data of [ $^{18}\text{F}$ ]-**1** in male Wistar rats are presented in Table 1. The data were obtained at 5 and 60 min post-injection (p.i), after intravenous bolus injection of the radiotracer. At early post-injection times, it was observed a moderately fast clearance of the  $^{18}\text{F}$ -radioactivity from the blood compartment with a value of  $0.49\pm 0.20\%$  ID/g at 5 min p.i. The percentages of injected dose (ID) that were found in the liver ( $4.83\pm 2.16\%$  at 5 min p.i. and  $2.38\pm 0.28\%$  at 60 min p.i.) and intestine

(5.30±2.63% at 5 min p.i. and 13.66±1.90% at 60 min p.i.) indicate a significant contribution of hepatobiliary excretion, as expected for a lipophilic compound. [<sup>18</sup>F]-**1** presents a calculated octanol/water partition coefficient (log P<sub>o/w</sub>) of 4.01, as we have reported previously (Ribeiro Morais, Miranda et al. 2011). [<sup>18</sup>F]-**1** has shown a moderate initial brain uptake (0.61±0.26 %ID/g at 5 min p.i.), which is consistent with its lipophilicity. The activity retained in the brain was 0.45±0.04 %ID/g, 60 min after i.v. administration (Fig. 3). Therefore, [<sup>18</sup>F]-**1** undergoes a relatively slow brain washout (5-to-60 min ratio = 1.36) in normal rat, which is a non favorable behavior for a specific radioprobe targeted at Aβ aggregates. In addition, [<sup>18</sup>F]-**1** showed a significant femur uptake (0.50±0.21 %ID/g at 5 min p.i.; 0.75±0.13 %ID/g at 60 min p.i.) that increased with time (Fig. 3), indicating the occurrence of *in vivo* defluorination. *In vivo* defluorination has been recently reported for related <sup>18</sup>F-labeled styryltriazone derivatives carrying also the radioactive label at an aliphatic sp<sup>3</sup> carbon atom (Lee, Choe et al. 2012).

**Table 1.**

**Figure 3.**

**Figure 4.**

The observed slow brain washout and increasing femur uptake indicated that [<sup>18</sup>F]-**1** was not stable *in vivo*, undergoing probably defluorination processes. To have a further insight into this point, we have performed radio-HPLC analysis of blood plasma from Wistar rats injected with [<sup>18</sup>F]-**1**. This study confirmed that [<sup>18</sup>F]-**1** was rapidly metabolized into a polar metabolite (see Supporting Information), being depicted in Fig. 4 the variation of the metabolite fraction over time. After 30 min p.i., the plasma

activity was due almost exclusively to the metabolite, which indicates that [ $^{18}\text{F}$ ]-**1** has a poor *in vivo* stability.

#### 4. Conclusions

A novel radiofluorinated styryl-benzoxazole derivative ([ $^{18}\text{F}$ ]-**1**) targeted at A $\beta$  aggregates has been synthesized in good yield and with high radiochemical purity and specific activity. Biodistribution and metabolism studies in rat have shown that this newly synthesized radiotracer can cross the BBB but displays a rather slow brain washout. Moreover, [ $^{18}\text{F}$ ]-**1** suffers extensive metabolization/defluorination *in vivo* and, therefore, is not a suitable radioprobe for *in vivo* imaging of A $\beta$  deposits in AD-affected brain. To overcome these drawbacks, we envisage to explore the use of different aliphatic linkers between the -CH<sub>2</sub><sup>18</sup>F group and the phenyl ring, as it has been reported that such linkers can strongly influence the *in vivo* stability of this type of compounds (Lee, Choe et al. 2012).

#### Acknowledgments

This work was funded by Fundação para a Ciência e Tecnologia (FCT), Portugal (PTDC/QUI/102049/2008). GRM thanks the FCT for the ‘Ciência 2008’ program and DAAD program (0811983). The research was carried out within the framework of the European Cooperation COST Action TD1007 (Bimodal PET-MRI molecular imaging technologies and applications for *in vivo* monitoring of disease and biological processes).

## References

- Bacskaï, B. J., G. A. Hickey, et al. (2003). "Four-dimensional multiphoton imaging of brain entry, amyloid binding, and clearance of an amyloid-beta ligand in transgenic mice." *Proc Natl Acad Sci U S A* **100**(21): 12462-12467.
- Barthel, H., H. J. Gertz, et al. (2011). "Cerebral amyloid-beta PET with florbetaben (F-18) in patients with Alzheimer's disease and healthy controls: a multicentre phase 2 diagnostic study." *Lancet Neurology* **10**(5): 424-435.
- Choi, S. R., G. Golding, et al. (2009). "Preclinical Properties of F-18-AV-45: A PET Agent for A beta Plaques in the Brain." *Journal of Nuclear Medicine* **50**(11): 1887-1894.
- Clark, C. M., J. A. Schneider, et al. (2011). "Use of florbetapir-PET for imaging beta-amyloid pathology." *JAMA* **305**(3): 275-283.
- Coenen, H. H., B. Klatte, et al. (1986). *J. Label Compd Radiopharm* (23): 455-463.
- Irvine, G. B., O. M. El-Agnaf, et al. (2008). "Protein aggregation in the brain: The molecular basis for Alzheimer's and Parkinson's diseases." *Molecular Medicine* **14**(7-8): 451-464.
- Jureus, A., B. M. Swahn, et al. (2010). "Characterization of AZD4694, a novel fluorinated A beta plaque neuroimaging PET radioligand." *Journal of Neurochemistry* **114**(3): 784-794.
- Klunk, W. E., H. Engler, et al. (2004). "Imaging brain amyloid in Alzheimer's disease with Pittsburgh Compound-B." *Annals of Neurology* **55**(3): 306-319.
- Kung, H. F. (2012). "The beta-Amyloid Hypothesis in Alzheimer's Disease: Seeing Is Believing." *Acs Medicinal Chemistry Letters* **3**(4): 265-267.
- Lee, I., Y. S. Choe, et al. (2012). "Synthesis and Evaluation of F-18-Labeled Styryltriazone and Resveratrol Derivatives for beta-Amyloid Plaque Imaging." *Journal of Medicinal Chemistry* **55**(2): 883-892.
- Liu, J., V. Kepe, et al. (2007). "High-yield, automated radiosynthesis of 2-(1-{6-[(2-[F-18]fluoroethyl)(methyl)amino]-2-naphthyl}ethylidene)malononitrile ([F-18]FDDNP) ready for animal or human administration." *Mol Imag Biol* **9**(1): 6-16.
- Liu, Y. J., L. Zhu, et al. (2010). "Optimization of automated radiosynthesis of [F-18]AV-45: a new PET imaging agent for Alzheimer's disease." *Nuclear Medicine and Biology* **37**(8): 917-925.
- Ribeiro Morais, G., H. V. Miranda, et al. (2011). "Synthesis and in vitro evaluation of fluorinated styryl benzazoles as amyloid-probes." *Bioorg Med Chem* **19**(24): 7698-7710.
- Ribeiro Morais, G., A. Paulo, et al. (2012). "A Synthetic Overview of Radiolabeled Compounds for ss-Amyloid Targeting." *European Journal of Organic Chemistry* (7): 1279-1293.
- Vandenberghe, R., K. Van Laere, et al. (2010). "F-18-Flutemetamol Amyloid Imaging in Alzheimer Disease and Mild Cognitive Impairment A Phase 2 Trial." *Annals of Neurology* **68**(3): 319-329.

## List of captions

### Figures:

- Figure 1.** Chemical structure of relevant A $\beta$  binding agents.
- Figure 2.** HPLC profile compound [ $^{18}\text{F}$ ]-1 (radiometric detection) with the assignment of its *E* and *Z* isomers.
- Figure 3.** Brain and femur uptake of [ $^{18}\text{F}$ ]-1 as a function of time.
- Figure 4.** Metabolite fraction in the blood plasma from a Wistar rat injected with [ $^{18}\text{F}$ ]-1

### Tables:

- Table 1.** Biodistribution results of [ $^{18}\text{F}$ ]-1 in male Wistar rat at 5 and 60 min after i.v. administration, expressed in %ID/organ  $\pm$  SD or %ID/g tissue  $\pm$  SD (n =7-8).

### Schemes:

- Scheme 1.** Retrosynthetic approach for the preparation of fluorinated styryl benzazoles(Ribeiro Morais, Miranda et al. 2011).
- Scheme 2.** Synthesis of [ $^{18}\text{F}$ ]-1 using aliphatic nucleophilic radiofluorination.

## Figures and schemes

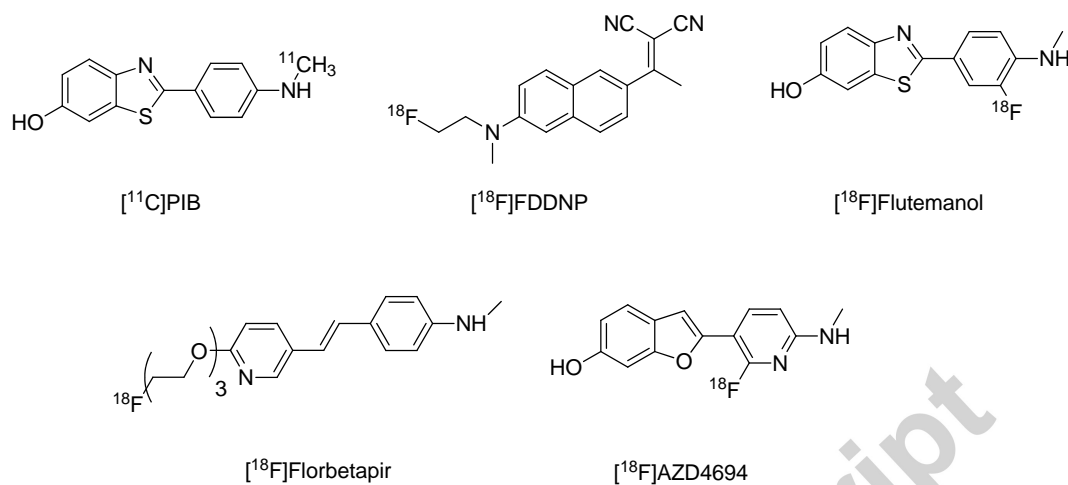
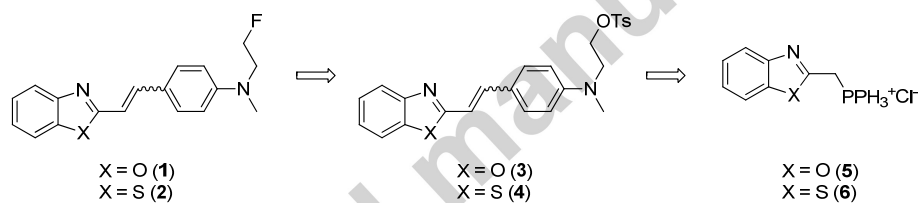
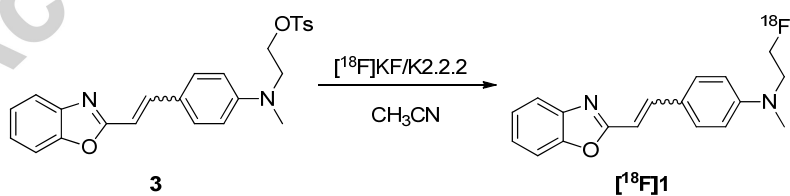


**Figure 1.** Chemical structure of relevant A $\beta$  binding agents.



**Scheme 1.** Retrosynthetic approach for the preparation of fluorinated styryl benzazoles (Ribeiro Morais, Miranda et al. 2011).



**Scheme 2.** Synthesis of [ $^{18}\text{F}$ ]-1 using aliphatic nucleophilic radiofluorination.

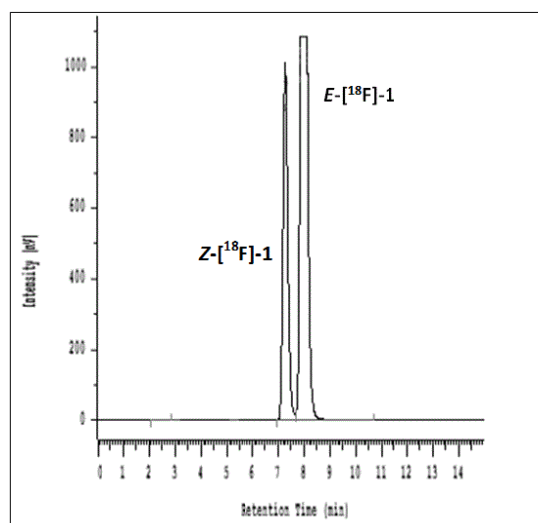


**Figure 2.** HPLC profile compound [<sup>18</sup>F]-1 (radiometric detection) with the assignment of its *E* and *Z* isomers.

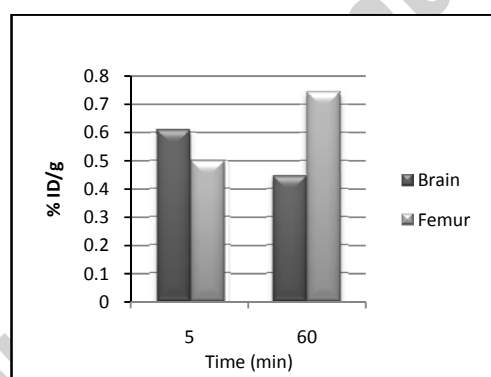


**Figure 3.** Brain and femur uptake of [<sup>18</sup>F]-1 as a function of time.

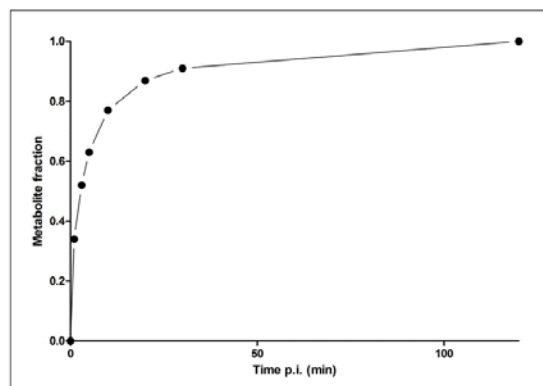


**Figure 4.** Metabolite fraction in the blood plasma from a Wistar rat injected with [ $^{18}\text{F}$ ]-  
1

#### Highlights

- Design of a fluorinated styryl benzoxazole derivative for detection of  $\beta$ -amyloid plaques.
- Nucleophilic radiofluorination with readily available [ $^{18}\text{F}$ ]KF.
- Metabolism and biodistribution studies of the radiofluorinated styryl benzoxazole derivative.